

RESEARCH ARTICLE

10.1002/2013JG002565

Key Points:

- Reconstructed 170-year spring phenology index for eastern China
- Significant trend of SPI of -4.1 days/decade in the most recent 30-year period
- SPI series correlates significantly with spring temperatures in the study area

Correspondence to:

J. Dai and H. Wang,
daijh@igsnr.ac.cn;
wang_huanjong@sina.com

Citation:

Ge, Q., H. Wang, J. Zheng, R. This, and J. Dai (2014), A 170 year spring phenology index of plants in eastern China, *J. Geophys. Res. Biogeosci.*, 119, 301–311, doi:10.1002/2013JG002565.

Received 11 NOV 2013

Accepted 14 FEB 2014

Accepted article online 17 FEB 2014

Published online 19 MAR 2014

A 170 year spring phenology index of plants in eastern China

Quansheng Ge¹, Huanjong Wang^{1,2}, Jingyun Zheng¹, Rutishauser This³, and Junhu Dai¹
¹Institute of Geographical Sciences and Natural Resources Research, Chinese Academy of Sciences, Beijing, China,

²University of Chinese Academy of Sciences, Beijing, China, ³Oeschger Centre for Climate Change Research (OCCR) and Institute of Geography, University of Bern, Bern, Switzerland

Abstract Extending phenological records into the past is essential for the understanding of past ecological change and evaluating the effects of climate change on ecosystems. A growing body of historical phenological information is now available for Europe, North America, and Asia. In East Asia, long-term phenological series are still relatively scarce. This study extracted plant phenological observations from old diaries in the period 1834–1962. A spring phenology index (SPI) for the modern period (1963–2009) was defined as the mean flowering time of three shrubs (first flowering of *Amygdalus davidiana* and *Cercis chinensis*, 50% of full flowering of *Paeonia suffruticosa*) according to the data availability. Applying calibrated transfer functions from the modern period to the historical data, we reconstructed a continuous SPI time series across eastern China from 1834 to 2009. In the recent 30 years, the SPI is 2.1–6.3 days earlier than during any other consecutive 30 year period before 1970. A moving linear trend analysis shows that the advancing trend of SPI over the past three decades reaches upward of 4.1 d/decade, which exceeds all previously observed trends in the past 30 year period. In addition, the SPI series correlates significantly with spring (February to April) temperatures in the study area, with an increase in spring temperature of 1°C inducing an earlier SPI by 3.1 days. These shifts of SPI provide important information regarding regional vegetation-climate relationships, and they are helpful to assess long term of climate change impacts on biophysical systems and biodiversity.

1. Introduction

The impacts of climate change have become increasingly noticeable in various biological and physical systems over the last several decades [Rosenzweig et al., 2008]. The phenology, physiology, and distribution of plant species are very sensitive to climate, and their changes have been observed all over the world in the last 30 years [Intergovernmental Panel on Climate Change, 2007; Walther, 2003]. The shifts of plant phenology, in particular, alter the timing of vegetation activity and might further influence regional and global carbon cycles [Churkina et al., 2005; Peñuelas et al., 2004]. Moreover, phenological change has important implications not only for biodiversity [Both et al., 2006] and food supply [Mémott et al., 2007] but also for climate change through biophysical feedback [Peñuelas et al., 2009].

Over the past several decades, shifts in plant phenology as monitored at the species level through observation networks have shown a significant trend toward earlier onsets of spring in Europe [Menzel, 2000; Menzel et al., 2006], North America [Abu-Asab et al., 2001; Beaubien and Freeland, 2000], East Asia [Doi, 2012; Ho et al., 2006; Wang et al., 2012], and Australia [Webb et al., 2011]. In many cases, the timing of the spring phases for multiple species corresponds greatly with one another [Hameed and Gong, 1994; Rutishauser et al., 2007]. Similarly, the integrated green onset dates derived from satellite data on a landscape scale also indicated advancing trends in most parts of the world [Jeong et al., 2011; Liang et al., 2011; Studer et al., 2007]. However, delays of budburst/leaf out due to the interaction of chilling requirements and warming temperatures are also found in some temperate tree species [Körner and Basler, 2010]. Also, vegetation green onset date derived from satellite data has been delayed in some high-latitude regions [Zhang et al., 2007].

The phenological shifts are attributed to changes in climate [Jolly et al., 2005; Stöckli et al., 2011] and linked to atmospheric circulation indices (e.g., North Atlantic Oscillation or Arctic Oscillation) [Buermann et al., 2003; Menzel, 2003] or surface temperature [Cleland et al., 2006]. Photoperiod is also a key factor controlling phenology [Basler and Körner, 2012; Caffarra and Donnelly, 2011]. In specific biomes, other influencing factors of phenology may play a pivotal role; e.g., the effect of precipitation on the phenology of plants is obvious in arid and semiarid areas [Du et al., 2010; Gibbens, 1991] or in tropical ecosystems [Reich, 1995].

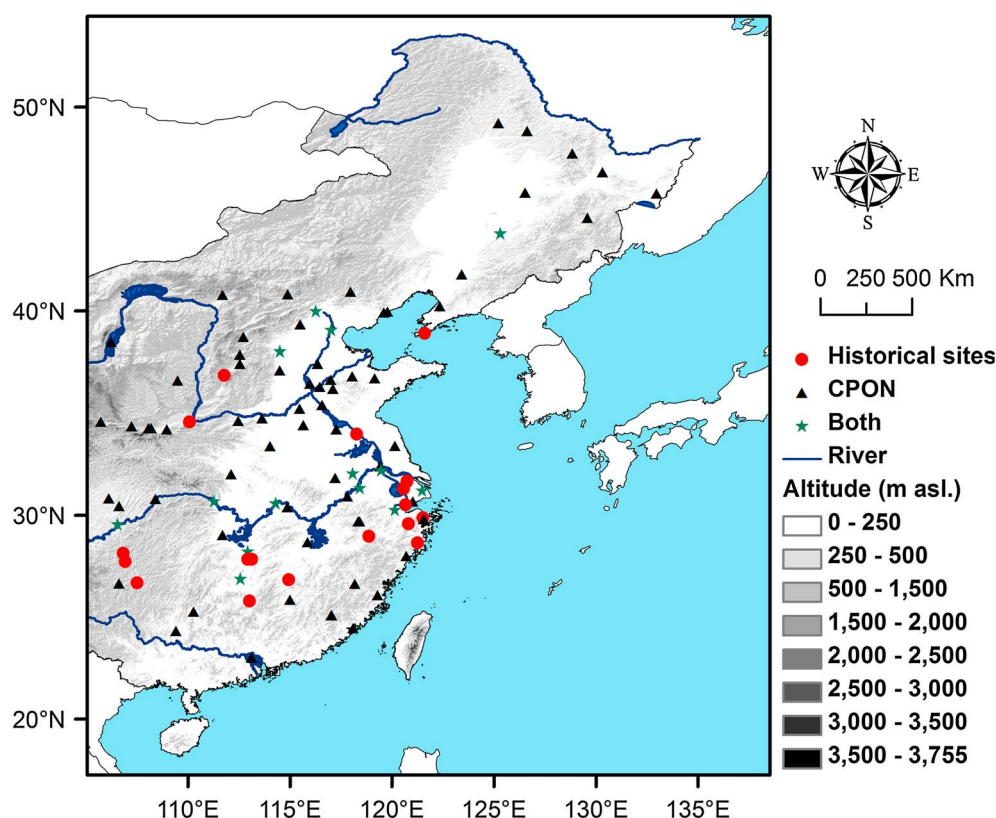


Figure 1. Locations of phenological observation sites: Chinese Phenological Observation Network (1963–2009) and historical documents.

In temperate zones, temperature is the dominant cue of the start of the growing season [Caldararu *et al.*, 2014; Wilczek *et al.*, 2010]. In terms of unprecedented temperature rise and associated phenological trends in recent decades, long-term and continuous phenological series are essential for studies of decadal to centennial time scales. So far, however, most phenological studies have focused on the second half of the 20th century, which is mainly due to the lack of availability of long-term data. Only several long-term phenological series (more than 100 years) are available in Europe [Ahas, 1999; Chuine *et al.*, 2004; Rutishauser *et al.*, 2007; Schaber and Badeck, 2005], Japan [Aono and Kazui, 2008], and the U.S. [Miller-Rushing and Primack, 2008]. In China, a few studies have investigated multicentury phenological series [Ge *et al.*, 2003; Gong *et al.*, 1984; Hameed and Gong, 1994; Zheng *et al.*, 2013]; however, as far as the completeness of these series and the size of their study area are concerned, they are either discontinuous or spatially quite limited. Therefore, only very limited independent evidence exists that assesses the continuous process of climate impacts on vegetation dynamics, especially in China.

To address this shortcoming, and extend the phenological series, we used a statistical approach to reconstruct a 170 year long, annually resolved spring phenological data series for eastern China. We obtained these phenological data from historical documents (i.e., journals and diaries) as well as from ground observations from the Chinese Phenological Observation Network (CPON). These data enabled us to define a spring phenology index (SPI) using the mean flowering times of three woody plants. Subsequently, we reconstructed the annual SPI through the transfer function of respective phenophases. The objectives of the present study were to reconstruct a long-term phenological series by combining modern network observations with data derived from historical archives. The reconstructed SPI also provides new evidence to assess vegetation-climate interactions for a less studied area.

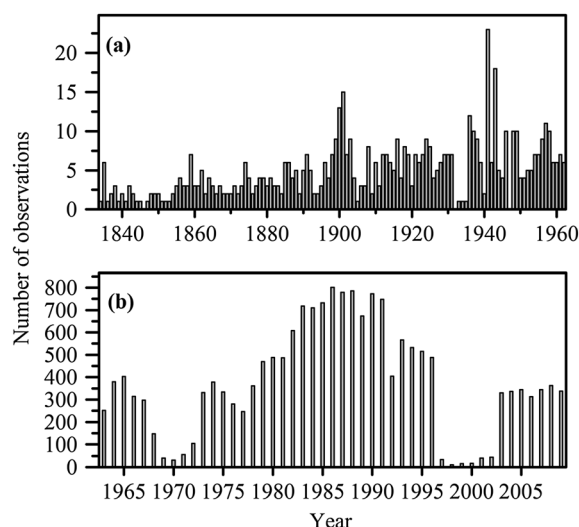


Figure 2. The number of observations used in the study for each year. (a) Historical observations. (b) CPON

2000 mm in the southeast to 150 mm in the northwest. The major biomes involved in the study area from north to south are cool temperate deciduous needleleaf forest, temperate mixed needleleaf and deciduous broadleaf forest, warm temperate deciduous broadleaf forest, and subtropical broadleaf evergreen forest [Editorial Committee of Vegetation Map of China, Chinese Academy of Sciences, 2007].

2.2. Phenological Observations

In the modern period of the study (1963–2009), we used phenological data from the Chinese Phenological Observation Network, which is administrated through the sponsorship of the Chinese Academy of Sciences. A total of 81 sites in the CPON overlap with the same area as the historical observations (Figure 1). These sites took more than 100 observations per year except for two specific periods (Figure 2b). The first of these two exceptions occurred at the time of the broad social upheavals of the Cultural Revolution (1969–1972), and the second occurred between 1997 and 2002 with limited funding for the CPON. During these two periods, only 10–40 observations per year were recorded.

For the historical period covered by this study (1834–1962), a total of 618 phenological observations in 129 years were available. These observations were made prior to the development of the modern phenological network and were extracted primarily from 20 diaries (dating back to the late Qing Dynasty). In Chinese culture, scholars in history regularly kept personal diaries recording important events as they happened, including accounts of daily weather conditions and seasonal plant events. Especially important were events related to popular decorative plant species. Thus, these dairies contain a lot of phenological information. For example, in 1885, Liewen Zhao, who was an assistant to a general living in Beijing, recorded the following observation in his “diary of Nengjing JU”: “9 March, clear sky, Chinese plum (*Prunus mume*) begun to blossom; 18 March, clear sky, Chinese plum in the garden is fully blossom. My whole family admired the beauty of flowers.” Although such historical observations were not strictly gathered according to modern, systematic guidelines, numerous studies to date have concluded that these phenological observations were often personally motivated and contain reliable information [Aono and Kazui, 2008; Rutishauser *et al.*, 2007; Rutishauser, 2009; Zhu, 1973]. Therefore, such historical phenological observations have been recognized as one of the reliable proxies for reconstructing historical climate in Europe and China [Brázdil *et al.*, 2005; Ge *et al.*, 2003].

In the data from both the historical diaries and the modern CPON, 19 species of deciduous woody plants and nine phases (e.g., first flowering, 50% of full flowering, and end of flowering) were analyzed (Table 1). The total analysis therefore amounted to 57 spring phenophases, with one phenophase representing a single phase for a specific species, distributed at 100 sites across eastern China (Figure 1 and Table 1). Before 1897, less than 5 observations per year were available thereafter usually more than 5–10 observations per year (Figure 2a). For all available historical data, 300 observations had already been acquired by previous studies

2. Materials and Methods

2.1. Study Area

The study region covers eastern China (Figure 1). Eastern China covers a large geographic area of 3500 km from southwest to northeast of the study area. The study area has a complicated terrain and mainly consists of three plateaus (the inner Mongolian, the Loess, and the Yunnan-Guizhou Plateaus) with elevations between 1000 and 2000 m above sea level (asl) and three plains (the Northeast China Plain, the North China Plain, and the middle-lower Yangtze Plain) with elevations less than 100 m asl. Most parts of eastern China have a monsoon climate with hot, humid summers and cold, arid winters. The mean annual temperature from north to south of the entire study area ranges from -4 to 24°C . The mean annual precipitation decreases from

Table 1. The Parameters of Transfer Functions and Reconstruction Accuracy for Individual Phenophases for the Estimation of the SPI

No.	Species	Phases ^a	N ^b	Parameters		Reconstruction Accuracy		
				d^c	e^c	R^{2d}	RMSE ^e	RE ^f
1	<i>Amygdalus persica</i> f. <i>duplex</i> Rehd.	FF	38	0.61	41.47	0.46	3.39	0.45
2	<i>Amygdalus persica</i> f. <i>duplex</i> Rehd.	50 F	33	0.56	42.66	0.26	3.49	0.25
3	<i>Chaenomeles speciosa</i>	FF	32	0.55	52.10	0.77	2.43	0.77
4	<i>Chaenomeles speciosa</i>	50 F	27	0.59	45.61	0.64	2.84	0.63
5	<i>Chaenomeles speciosa</i>	EF	26	0.60	36.32	0.28	3.99	0.28
6	<i>Robinia pseudoacacia</i>	FF	47	0.98	−19.58	0.70	2.79	0.70
7	<i>Robinia pseudoacacia</i>	50 F	44	0.94	−17.56	0.68	2.69	0.68
8	<i>Robinia pseudoacacia</i>	EF	42	0.82	−8.95	0.50	3.40	0.50
9	<i>Pyrus</i> sp.	FF	24	0.54	49.74	0.39	3.37	0.39
10	<i>Pyrus</i> sp.	50 F	22	0.52	50.33	0.25	3.85	0.23
11	<i>Pyrus</i> sp.	EF	22	0.55	42.55	0.33	3.20	0.31
12	<i>Prunus salicina</i>	FF	35	0.55	41.98	0.34	3.58	0.33
13	<i>Prunus salicina</i>	50 F	35	0.53	42.26	0.20	4.36	0.19
14	<i>Prunus salicina</i>	EF	33	0.50	42.12	0.25	3.85	0.24
15	<i>Salix babylonica</i>	FL	42	0.57	54.90	0.55	3.10	0.55
16	<i>Salix babylonica</i>	50 L	41	0.43	61.90	0.36	3.82	0.33
17	<i>Salix babylonica</i>	BB	41	0.45	68.82	0.31	3.89	0.30
18	<i>Salix babylonica</i>	FF	41	0.71	36.15	0.52	3.22	0.52
19	<i>Salix babylonica</i>	50 F	42	0.74	31.39	0.64	2.82	0.64
20	<i>Salix babylonica</i>	EF	41	0.72	28.71	0.67	2.66	0.67
21	<i>Salix babylonica</i>	FD	39	0.49	41.52	0.57	2.86	0.57
22	<i>Prunus mume</i>	FF	34	0.23	85.94	0.22	3.86	0.22
23	<i>Prunus mume</i>	50 F	34	0.30	78.78	0.38	3.45	0.37
24	<i>Prunus mume</i>	EF	34	0.30	74.97	0.28	3.72	0.27
25	<i>Paeonia suffruticosa</i>	FF	44	0.85	5.48	0.77	2.45	0.77
26	<i>Paeonia suffruticosa</i>	50 F	47	0.93	−7.65	0.75	2.57	0.75
27	<i>Paeonia suffruticosa</i>	EF	41	0.75	6.64	0.60	3.07	0.60
28	<i>Cerasus yedoensis</i>	FF	43	0.47	53.10	0.62	2.89	0.62
29	<i>Cerasus yedoensis</i>	50 F	41	0.51	47.45	0.66	2.53	0.66
30	<i>Cerasus yedoensis</i>	EF	39	0.39	55.46	0.38	3.38	0.37
31	<i>Amygdalus davidiana</i>	FF	47	0.79	29.96	0.73	2.67	0.72
32	<i>Amygdalus davidiana</i>	50 F	46	0.80	25.65	0.71	2.76	0.71
33	<i>Amygdalus davidiana</i>	EF	44	0.79	19.45	0.64	3.06	0.64
34	<i>Amygdalus persica</i>	FF	41	0.61	46.04	0.52	3.23	0.52
35	<i>Amygdalus persica</i>	50 F	41	0.72	32.60	0.49	3.32	0.49
36	<i>Amygdalus persica</i>	EF	40	0.72	27.33	0.44	3.22	0.44
37	<i>Malus micromalus</i>	FF	43	0.58	40.83	0.61	2.99	0.59
38	<i>Malus micromalus</i>	50 F	42	0.56	39.32	0.41	3.66	0.41
39	<i>Malus micromalus</i>	EF	41	0.76	13.25	0.67	2.74	0.66
40	<i>Armeniaca vulgaris</i>	FF	45	0.76	30.33	0.69	2.64	0.69
41	<i>Armeniaca vulgaris</i>	50 F	43	0.86	18.67	0.76	2.55	0.76
42	<i>Armeniaca vulgaris</i>	EF	42	0.89	8.90	0.71	2.62	0.71
43	<i>Cerasus pseudocerasus</i>	FF	22	0.51	43.62	0.31	2.69	0.30
44	<i>Cerasus pseudocerasus</i>	50 F	22	0.49	46.72	0.23	2.86	0.21
45	<i>Ulmus Pumila</i>	FM	39	0.89	−6.24	0.61	2.73	0.61
46	<i>Magnolia denudata</i>	FF	44	0.56	57.60	0.66	2.74	0.66
47	<i>Magnolia denudata</i>	50 F	42	0.65	46.89	0.77	2.23	0.77
48	<i>Magnolia denudata</i>	EF	41	0.71	35.83	0.77	2.29	0.77
49	<i>Syringa oblata</i>	FF	46	0.73	20.07	0.63	3.11	0.63
50	<i>Syringa oblata</i>	50 F	44	0.71	19.10	0.57	3.35	0.57
51	<i>Syringa oblata</i>	EF	41	0.81	−0.83	0.44	3.63	0.44
52	<i>Cercis chinensis</i>	FF	47	0.67	39.23	0.87	1.86	0.87
53	<i>Cercis chinensis</i>	50 F	45	0.67	35.72	0.86	1.91	0.86
54	<i>Cercis chinensis</i>	EF	42	0.72	22.07	0.74	2.69	0.73
55	<i>Wisteria sinensis</i>	FF	44	0.71	24.22	0.80	2.27	0.80
56	<i>Wisteria sinensis</i>	50 F	44	0.73	19.23	0.77	2.47	0.77
57	<i>Wisteria sinensis</i>	EF	42	0.48	41.52	0.45	3.71	0.40

^aPhases: FF: first flowering; 50 F: 50% of full flowering; EF: end of flowering; FL: first leaf; 50 L: 50% of full leaf expansion; BB: bud burst; FM: fruit maturity; FD: fruit drop.

^bN: number of years with observation data between 1963 and 2009.

^c d and e : parameters of transfer functions (equation (4)).

^d R^2 : variance of SPI explained by respective single phenophases.

^eRMSE: root-mean-square error of cross-validated SPI reconstruction.

^fRE: reduction of the error of cross-validated SPI reconstruction.

[Fang et al., 2005; Gong et al., 1984; Hameed and Gong, 1994; Zheng et al., 2013]. These studies focused on a specific location (e.g., Beijing) or a small area (e.g., Beijing or Yangtze River Delta) and generate discontinuous series. Based on these studies, we acquired 318 additional phenological observations for this study from archival sources.

For validation and interpretation, we have compared our reconstructed spring phenological series with the long-term temperature data in eastern China (Figure 1). We chose the Climatic Research Unit Temperature version 4 (CRUTEM4) data set (<http://www.cru.uea.ac.uk/cru/data/temperature/>), which provides reliable global grid box data set of 5° latitude × 5° longitude temperature anomalies [Jones et al., 2012; Morice et al., 2012]. After averaging the temperature from the CRUTEM4 on grids representing eastern China, monthly mean temperature anomalies from 1850 to 2009 were obtained.

Moreover, we compared the spring phenological series in this study with the observed phenological series for Switzerland [Rutishauser et al., 2007] and Japan [Aono and Kazui, 2008; Aono and Saito, 2010]. For Switzerland, the phenological series we used is a reconstruction of a statistical “Spring plant” defined as the weighted mean for the flowering of cherry (*Prunus avium*) and apple (*Malus domestica*) tree and budburst of beech (*Fagus sylvatica*) from 1702 to 2009 [Rutishauser et al., 2007]. For Japan, the phenological series we chose is the full flowering dates of Japanese cherry (*Prunus jamasakura*) at Kyoto from 801 to 2009 [Aono and Saito, 2010].

2.3. Reconstruction Method

2.3.1. Combination of Phenological Time Series

Fragmentary phenological information are available at many observational sites. First, we combined the observation of each phenophase at different sites to form a continuous, regional species-specific time series. Following [Häkkinen et al., 1995; Schaber and Badeck, 2002] the combined time series y_i ($i = 1, 2, \dots, M$, where M is the total number of years) can be defined as

$$y_i = \frac{1}{n_i} \sum_{j=1}^{n_i} (x_{ij} - b_j) \quad (1)$$

where y_i is the regional averages of the observations x_{ij} of year i at station j , adjusted by b_j . The variable b_j is the site effect, which is mainly determined by geographic factors (i.e., latitude, longitude, and altitude). The variable n_i is the number of observations, and N is the total number of stations considered. The variable $n_i \leq N$ because some x_{ij} are undefined due to the problem that no observations were carried out in year i at station j . The optimal value of b_j can be estimated by an iterative optimization algorithm that minimizes the sum of squared residuals (S):

$$S = \sum_i \sum_j (x_{ij} - b_j - y_i)^2 \quad (2)$$

The minimum of S is found by differentiating S with respect to b_j and y_i and setting the resulting derivatives equal to zero. Meanwhile, we impose $\sum_{j=1}^N b_j = 0$ to obtain a unique solution of b_j and y_i (see Schaber and Badeck [2002] for more details).

For the period 1963–2009, the combined series y_i for each phenophase can be calculated according to the methods described above (similar method was also used for historical phenological observations; see section 2.3.4). In this way, the corresponding site effects in all the distribution sites (b_j) for each phenophase is obtained.

2.3.2. Definition of the Spring Phenology Index

Second, the spring phenology index can be defined as

$$\text{SPI} = \frac{1}{n} \sum_{l=1}^n y_l \quad (3)$$

where y_l is the combined series (1963–2009) of a specific phenophase l [Rutishauser et al., 2007]. We chose three phenophases ($n = 3$) covering the whole modern period (1963–2009; Table 1). The three phenophases are the first flowering of *Amygdalus davidiana* and *Cercis chinensis*, and 50% of the full flowering of *Paeonia suffruticosa* (*Robinia pseudoacacia* was not chosen because it is an exotic species). In this way, the SPI series from 1963 to 2009 can be calculated using equation (3).

Table 2. Mean Values of Parameters of Transfer Functions and Reconstruction Accuracy for Individual Phases^a

Phases	Number	d	e	R^2	RMSE	RE
FF	18	0.63	37.68	0.59	2.90	0.59
50 F	18	0.66	33.18	0.56	2.98	0.55
EF	16	0.66	27.83	0.51	3.20	0.50
BB	1	0.45	68.82	0.31	3.89	0.30
FL	1	0.57	54.90	0.55	3.10	0.55
50 L	1	0.43	61.90	0.36	3.82	0.33
MF	1	0.89	−6.24	0.61	2.73	0.61
FD	1	0.49	41.52	0.57	2.86	0.57
All phases	57	0.64	34.06	0.55	3.04	0.54

^aSee Table 1 for phases and label descriptions.

2.3.3. Transfer Functions Between SPI and Combined Series

Third, we calculated the combined series for all the selected phenophases in the period 1963–2009. We calibrated transfer functions between the SPI series and the combined series of each respective phenophase. The transfer function was a linear regression function with parameters d and e :

$$\text{SPI} = d|y| + e_l \quad (4)$$

For uncertainty estimates, we cross validated each phenophase-specific transfer function in the period 1963–2009 [Michaelsen, 1987]. Each year was withheld once from the data set, and the transfer function was performed with the retained years, then the SPI in the current year can be simulated. Finally, the simulated interannual SPI series was obtained. Subsequently, we calculated the root-mean-square error (RMSE) and reduction of error (RE) between the observed SPI and the simulated SPI for each phenophase. For the RE (equation (5)), an RE of +1 is a perfect reconstruction whereas an RE of 0 means a long-term average [Cook *et al.*, 1994; Rutishauser *et al.*, 2007]. RE values between −1 and 0 are better than random but worse than the long-term mean.

$$\text{RE} = 1 - \frac{\sum_{i=1}^M (\text{SPI}_i - \text{SPI}_{Ri})^2}{\sum_{i=1}^M (\text{SPI}_i - \text{SPI}_{\text{mean}})^2} \quad (5)$$

where SPI_i is the observed SPI in year i , SPI_{Ri} is the simulated SPI in year i derived from cross validation, SPI_{mean} is the mean SPI over the full period 1963–2009.

2.3.4. Reconstructions of Historical SPI

The following processes were conducted to reconstruct the historical SPI. First, for the historical period 1834–1962, we applied equation (1) to each historical observation to remove the site effect b_j . If phenophase was also recorded during 1963–2009 at the site j . The variable b_j can be known through the process of combining phenological time series. If the b_j is unknown, it can be estimated by a multiple regression equation between b_j and geographic factors (i.e., latitude, longitude, and altitude). Second, we applied the corresponding phenophase-specific transfer functions to the observation with the site effect removed. Consequently, the SPI in each historical year could be obtained by averaging all reconstructed SPIs in the same year.

We used a 10 year Gaussian filter to smooth the SPI series. Uncertainties for the SPI series were estimated using the mean RMSE of corresponding transfer functions from the calibration period 1963–2009. The temporal trends of SPI can be represented by the slopes of a linear regression between the SPI and the time (in year) calculated for each 30 year period by moving the center year with a step length of 1 year. The relationship between the SPI and temperature was also assessed using a simple linear regression.

3. Results

The individual phenophase clearly represents the interannual variability of the defined SPI (Table 1). All the phenophases investigated explain 23% to 83% of the variance of SPI with a mean of 55% (Tables 1 and 2). The RMSE is between 2.1 and 4.3 days, resulting in a mean reconstruction uncertainty of 3.04 days. RE values are all positive suggesting that the reconstruction has better skill than the long-term mean (Table 1). For

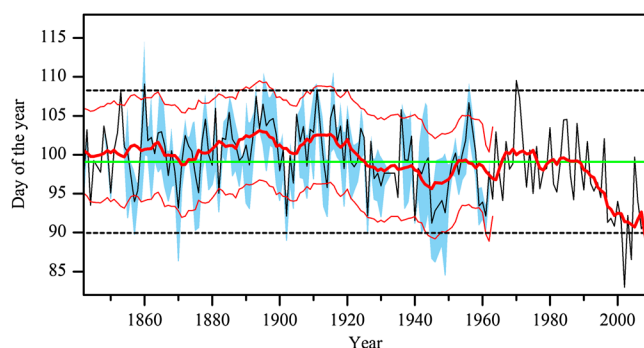


Figure 3. The spring phenology index for eastern China from 1834 to 2009. The 10 year moving window average shows decadal changes (bold red line) with associated uncertainties (2 RMSE, thin red line) due to the regression between the observed and reconstructed SPI (1963–2009). Confidence intervals due to different observations (standard deviation) are shaded in blue. The green horizontal line shows the long-term mean (9 April, day of year: 99) in the period 1843–2009 (note that this value is equal to the 1961–1990 mean). The dotted lines indicate the 2 standard deviation range of 9.3 days of the entire period (1843–2009). There are no observations in 1846, 1932, and 1947.

reproductive phenophases (flowering phenology), earlier phases have higher reconstruction accuracy than the later phases (Table 2).

The transfer functions applied to the historical observations to reconstruct the SPI back to 1834 are listed in Table 1. Based on this reconstruction, the mean SPI in the recent 29 years (1980–2009) indicates an earlier spring phenology than in any other 29 year period (Figure 3). In particular, the SPI are earlier than the 1961–1990 mean in most of the years after 1990. Similar conditions also arose during the period 1920–1950, though with higher uncertainties due to a smaller number of observations. The 10 year Gaussian filtered SPI series highlights the earlier and later decades (Figure 3). The 1940s, 1960s, 1990s, and 2000s experienced obvious earlier spring. Among these decades, the spring season in the 2000s was the earliest. Late periods occurred from the 1830s to the 1910s. And the 1890s and 1910s are the two periods on record in the past 170 years with latest spring.

The moving linear trends of the reconstructed SPI show a pronounced advancing trend of -4.1 d/decade for the most recent period 1970–2009 (Figure 4). With respect to the past 170 year, the 30 year period with the center year from 1918 to 1935 also show significantly negative trends of around -2 d/decade ($P < 0.05$), not exceeding the trend of the most recent decades. The number of significantly positive trends is less than the number of negative trends over the study period. Significantly delayed trends were only found for the 30 year period with center years 1880–1885 and 1957–1960 (Figure 4). In general, before 1980, the trends of SPI in any consecutive 30 year period stay within the range between -2.6 and 2.6 day decade $^{-1}$; however, the trends in the most recent 30 years show an unusual advancing trend that surpasses all previously observed trends in the past 30 year period.

The SPI correlated negatively and significantly with the January to April, February to April, March to April, and April averages of temperatures in eastern China (Figure 5). The correlation coefficient between SPI and the February to April temperature was strongest (Figure 5; Pearson's $R = -0.71$). The regression analysis suggests that the spring phenology in eastern China would advance by 3.1 days when the February to April temperature increases by 1°C . Figure 6 shows the inverted SPI and the February to April temperature for the last 160 years. We found that the general trends of these two variables are similar and that the spring temperature (T) can explain more than 50% of the SPI variation ($\text{SPI} = -3.12 T + 98.71$, $R^2 = 0.51$, $P < 0.001$).

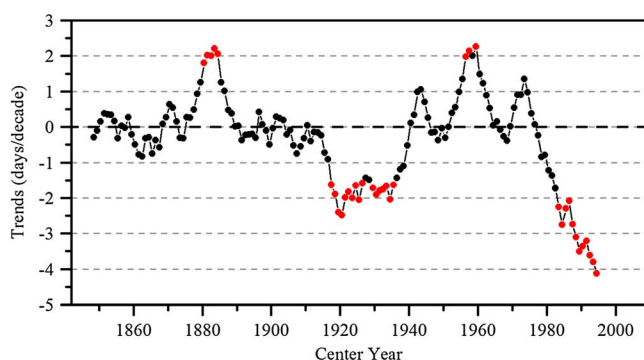


Figure 4. Thirty-year moving trends of the SPI for eastern China. The statistically significant trends ($P < 0.05$) are marked with red circle.

4. Discussion

From the methodological point of view, the method to maximize the use of phenological data is very crucial since the historical records often lie in multiple sites with many phenophases involved (Figure 1 and Table 1). To

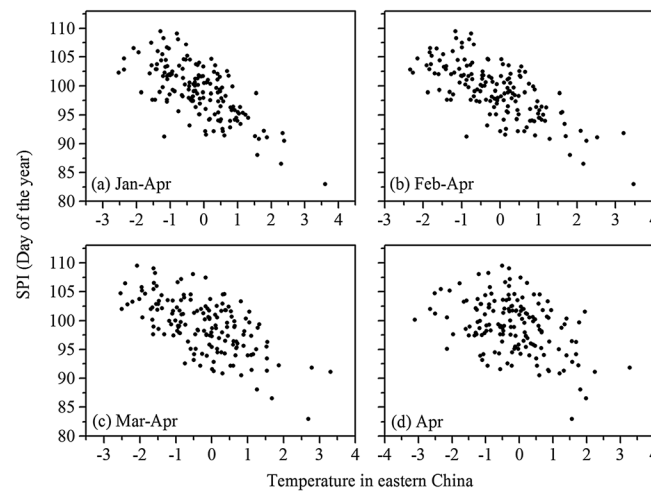


Figure 5. The relationship between the spring phenology index and the average of the eastern China temperature for (a) January to April (Pearson's $R = -0.70$, regression slope = $-3.2^{\circ}\text{C}^{-1}$; $P < 0.001$); (b) February to April (Pearson's $R = -0.71$, regression slope = $-3.1^{\circ}\text{C}^{-1}$, $P < 0.001$); (c) March to April (Pearson's $R = -0.63$, regression slope = $-2.7^{\circ}\text{C}^{-1}$, $P < 0.001$), and (d) April (Pearson's $R = -0.41$, regression slope = $-1.8^{\circ}\text{C}^{-1}$, $P < 0.001$).

provided a solution to the problem that long-term and continuous phenological series in eastern China were lacking. Consequently, we have the unique possibility to assess the extreme change in phenological time series in the long-term perspective. For example, in 1892, southeastern China experienced a very severe cold winter, many lakes (Tai Lake and Dongting Lake) and rivers (lower reaches of Huaihe, Huangpu, and Yangtze Rivers) freezeup with a long duration as recorded in Chinese historical documents [Zheng et al., 2012]. This extreme cold event can be related to the phenological extreme events of plants. As expected, the SPI in 1893 (17 April) was 8 days later than the 1960–1990 mean (9 April). However, the magnitude of this late spring event seems not unique in its amplitude. The spring in 1853, 1860, 1911, and 1970 was even later than in 1893. Throughout the record, the mid-1890s and late 1910s show a longer period of (consecutive 7–8 years) markedly later spring (Figure 3).

Since conclusions about the impact of climate change based on short-term observations can be misleading [Amano et al., 2010; Chuine et al., 2004], the 170 year index developed in this study provides a basis for

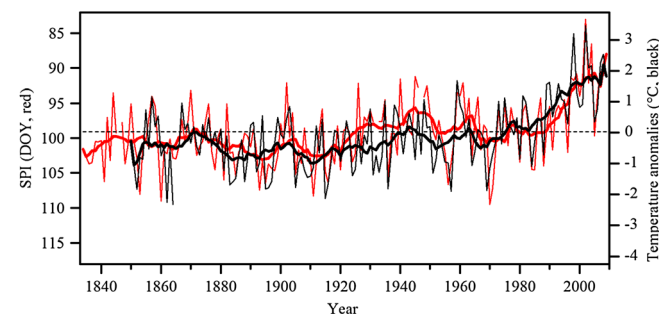


Figure 6. The spring phenology index (thin red line) and the February to April temperature (thin black line) derived from CRUTEM4 in eastern China. The SPI was inverted for clarity. The equation of linear regression between SPI and temperature (T) is $SPI = -3.12T + 98.71$ ($R^2 = 0.51$, $P < 0.001$). The dotted line shows the 1961–1990 mean. The 10 year moving window averages of SPI (bold red line) and temperature (bold black line) are plotted.

address this problem, on the one hand, we used the methodology proposed by Häkkinen et al. [1995] and Schaber and Badeck [2002] to remove the site effect of phenological observations and then generate a combined and regional phenological series. On the other hand, according to the processing step of Rutishauser et al. [2007], we calibrated the linear regression function between SPI and regional series of individual phenophases to solve the problem of integrating multiple phenophases. Building on this research, the approach adopted in this study has enabled us to maximize the use of phenological data among localities and species, and it also can be used to investigate previously unexamined areas.

Further, this study first reported a 170 year long and almost continuous (only missing 3 years) spring phenology index for eastern China. The results have

investigating whether the impact of recent climate change is unprecedented in the history. For example, the mid-1940s are exceptionally early for this entire 170 year time series, where for 4 years (1945, 1946, 1948, and 1949), spring was markedly earlier than most any year in the study (Figure 3). Even in the late 1990s and early 2000s, several years (e.g., in 1996 and 2000) had a later SPI than the mid-1940s. Therefore, recent extreme early spring has occurred in historical period. However, when investigating the phenological change on a longer time scale, we found the SPI in recent 9 years (2000–2009) is earliest and unprecedented. Also, the SPI series in the most recent 30 year is

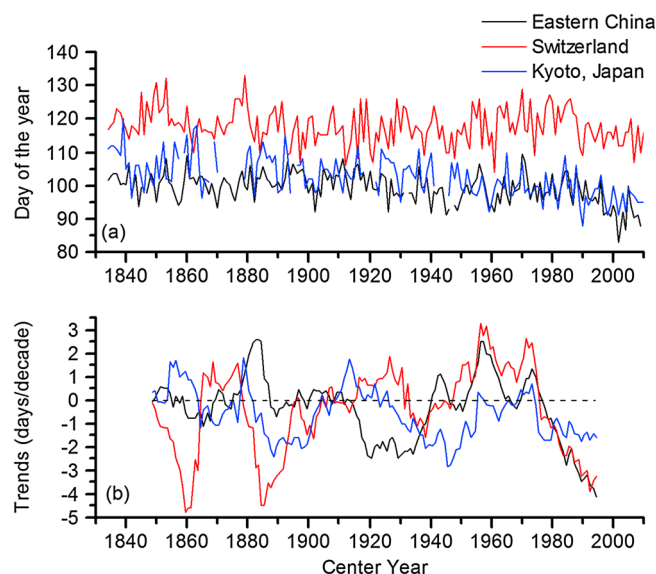


Figure 7. (a) The time series of the SPI in eastern China and statistical spring plant for the Swiss Plateau region [Rutishauser *et al.*, 2007] and full flowering time of Japanese cherry at Kyoto, Japan [Aono and Kazui, 2008; Aono and Saito, 2010]. (b) The time series of the 30 year moving trends of the above three spring indicators. The years with missing data in each data set are removed from all the three data sets when calculating the moving trends.

2.1–6.3 days earlier than in any other consecutive 30 year period from 1834 to 1970.

Similar with our results, other existing long-term series also indicated earlier spring in recent decades. For example, in Northern Finland, a cluster of the earliest springs could be found in the latest decades in the time series from 1750 to 2011 [Holopainen *et al.*, 2013]. In the UK, the estimated community level spring index in the most recent 25 years was 2.2–12.7 days earlier than any other consecutive 25 year period since 1760 [Amano *et al.*, 2010]. In the U.S., the record-breaking spring temperatures in 2010 and 2012 in Massachusetts and in 2012 in Wisconsin resulted in the earliest flowering times in recorded history for dozens of spring flowering plants of the eastern United States [Ellwood *et al.*, 2013].

All these findings including our

results are consistent with the instrumental temperature data, which show the more recent decades as the warmest from 1850 [Jones *et al.*, 2012].

Most of the changes in spring phenophases of plants can be directly related to rising late winter and spring temperature. The SPI series correlates significantly with the observed February to April temperatures in eastern China with an advance of $3.1 \text{ d}/^{\circ}\text{C}$ rise. The rate of advance in the SPI with temperature corresponds approximately to the range reported in different locations of Northern Hemisphere, e.g., 3.3 and $4.3\text{--}5.4 \text{ d}/^{\circ}\text{C}$ earlier flowering increase for Concord (in Massachusetts, USA) plants and for lilac in the western U.S., respectively [Cayan *et al.*, 2001; Miller-Rushing and Primack, 2008]; $5.0 \text{ d}/^{\circ}\text{C}$ earlier flowering increase for British plants [Amano *et al.*, 2010]; and mean advance of $2.5 \text{ d } ^{\circ}\text{C}^{-1}$ for phenophase of European plants [Menzel *et al.*, 2006]. Our result also fits well with finding in Japan, where the budburst date of *Ginkgo biloba* advanced by $2.9 \text{ d } ^{\circ}\text{C}^{-1}$ [Matsumoto *et al.*, 2003]. However, the temperature sensitivity ($-9 \text{ d } ^{\circ}\text{C}^{-1}$) of 19 Canadian plant species [Gonsamo *et al.*, 2013] based on short-term observation series (2000–2012) is about three times greater than our result.

The independent time series of SPI offers the means for comparisons with other spring indicators in different countries. Here we applied 30 year moving trends analysis to three independent spring indicators, including SPI, statistical spring plant for the Swiss Plateau region, and a long-term single phenological record (full flowering time of Japanese cherry) in Kyoto, Japan (Figure 7a). Three linear trend series show a general agreement in certain periods (Figure 7b). For the 1880s to 1890s, the spring indicators in Switzerland and Japan both have earlier trends, while the SPI in China show later trends. From 1950s to 1960s, the spring indicators in China and Switzerland show consistent later trends, while the trends in Japan are negative. In the 30 year period with center year after 1977, all the three indicators show consistent earlier trends. Overall, although the change of spring indicators has significant regional differences, a pronounced tendency toward earlier spring after the late 1970s can be found in all the three countries.

As shown in Figure 7a, several historical phenological series have been developed; however, the long-term indices that indicate the impact of climate change on ecosystems are still scarce [Walther *et al.*, 2002]. To our knowledge, there is no phenological index that has been officially adopted by the Chinese government. So the SPI series developed in this study can be adopted by policymakers for monitoring the impact of climate

change. Also, the SPI series could be used as an aid for the public alike to better understand the evidence provided by the plant world under the current rapid and ongoing climate change.

In the future, it will also be necessary to make good use of other Chinese historical literature to obtain further long-term phenological data series in other parts of China and in periods other than that covered in this study. Based on these newly reconstructed historical phenology indices, the relationship between climate variables and plant phenophases can be studied thoroughly. Furthermore, quantifying the impact of other climate parameters (e.g., precipitation and light or their interactive effects on phenology) and large-scale circulations is essential, as they could provide additional evidence on the joint effect of various factors.

5. Conclusions

Using more than 17,000 combined phenological observations of plants from historical documents and the CPON, this study first reported a 170 year long and almost continuous (only missing 3 years) spring phenology index for eastern China. The SPI in the recent 30 year is 2.0–6.3 days earlier than in any other consecutive 30 year period since 1834. The trend of spring phenology over the recent three decades (1980–2009) reaches up to -4.1 d/decade, which exceeds all previously observed trends. The SPI series correlates significantly with the observed spring (February to April) temperatures in eastern China with an advance of 3.1 d/°C rise. Therefore, temperature can be said to be the main driving factor of the spring season in eastern China. Overall, the SPI series provides new evidence of phenological responses to climate change in the Northern Hemisphere and can be the basis for further climate impact research in a long-term perspective.

Acknowledgments

This research was supported by the key project of the National Natural Science Foundation of China (NSFC) (41030101), the “Strategic Priority Research Program—Climate Change: Carbon Budget and Relevant Issues” of the Chinese Academy of Sciences (XDA05090301), NSFC project (41171043), and the National Basic Research Program of China (2012CB955304). Thanks to Gregory Pierce for his efforts in helping to smoothen the English language presentation of this paper and Yasuyuki Aono for providing the full flowering dates of Japanese cherry at Kyoto. We appreciate the comments of two anonymous reviewers that helped to improve the quality of the manuscript.

References

- Abu-Asab, M. S., P. M. Peterson, S. G. Shelter, and S. S. Orli (2001), Earlier plant flowering in spring as a response to global warming in the Washington, D. C., area, *Biodivers Conserv*, 10(4), 597–612.
- Ahas, R. (1999), Long-term phyt-, ornitho- and ichthyophenological time-series analyses in Estonia, *Int. J. Biometeorol.*, 42, 119–123.
- Amano, T., R. J. Smithers, T. H. Sparks, and W. J. Sutherland (2010), A 250-year index of first flowering dates and its response to temperature changes, *Philos Trans R. Soc B*, 277(1693), 2451–2457.
- Aono, Y., and K. Kazui (2008), Phenological data series of cherry tree flowering in Kyoto, Japan, and its application to reconstruction of springtime temperatures since the 9th century, *Int. J. Climatol.*, 28(7), 905–914.
- Aono, Y., and S. Saito (2010), Clarifying springtime temperature reconstructions of the medieval period by gap-filling the cherry blossom phenological data series at Kyoto, Japan, *Int. J. Biometeorol.*, 54(2), 211–219.
- Basler, D., and C. Körner (2012), Photoperiod sensitivity of bud burst in 14 temperate forest tree species, *Agric Forest Meteorol.*, 165, 73–81.
- Beaubien, E. G., and H. J. Freeland (2000), Spring phenology trends in Alberta, Canada: Links to ocean temperature, *Int. J. Biometeorol.*, 44(2), 53–59.
- Both, C., S. Bouwhuis, C. M. Lessells, and M. E. Visser (2006), Climate change and population declines in a long-distance migratory bird, *Nature*, 441(7089), 81–83.
- Brázdil, R., C. Pfister, H. Wanner, H. Von Storch, and J. R. Luterbacher (2005), Historical climatology in Europe: The state of the art, *Clim. Change*, 70(3), 363–430.
- Buermann, W., B. Anderson, C. J. Tucker, R. E. Dickinson, W. Lucht, C. S. Potter, and R. B. Myneni (2003), Interannual covariability in Northern Hemisphere air temperatures and greenness associated with El Niño-Southern Oscillation and the Arctic Oscillation, *J. Geophys. Res.*, 108(D13), 4396, doi:10.1029/2002JD002630.
- Caffarra, A., and A. Donnelly (2011), The ecological significance of phenology in four different tree species: Effects of light and temperature on bud burst, *Int. J. Biometeorol.*, 55, 711–721.
- Caldararu, S., D. W. Purves, and P. I. Palmer (2014), Phenology as a strategy for carbon optimality: A global model, *Biogeosciences*, 11, 763–778.
- Cayan, D. R., S. A. Kammerdiener, M. D. Dettinger, J. M. Caprio, and D. H. Peterson (2001), Changes in the onset of spring in the western United States, *Bull. Am. Meteorol. Soc.*, 82(3), 399–416.
- Chuine, I., P. Yiou, N. Viovy, B. Seguin, V. Daux, and E. L. R. Ladurie (2004), Historical phenology: Grape ripening as a past climate indicator, *Nature*, 432, 289–290.
- Churkina, G., D. Schimel, B. H. Braswell, and X. Xiao (2005), Spatial analysis of growing season length control over net ecosystem exchange, *Global Change Biol.*, 11(10), 1777–1787.
- Cleland, E. E., N. R. Chiariello, S. R. Loarie, H. A. Mooney, and C. B. Field (2006), Diverse responses of phenology to global changes in a grassland ecosystem, *Proc. Natl. Acad. Sci. U. S. A.*, 103(37), 13,740–13,744.
- Cook, E. R., K. R. Briffa, and P. D. Jones (1994), Spatial regression methods in dendroclimatology: A review and comparison of two techniques, *Int. J. Climatol.*, 14(4), 379–402.
- Doi, H. (2012), Response of the *Morus bombycis* growing season to temperature and its latitudinal pattern in Japan, *Int. J. Biometeorol.*, 56, 895–902.
- Du, J., P. Yan, Y. Dong, and F. Han (2010), Phenological response of *Nitraria tangutorum* to climate change in Minqin County, Gansu Province, northwest China, *Int. J. Biometeorol.*, 54(5), 583–593.
- Editorial Committee of Vegetation Map of China, Chinese Academy of Sciences (2007), *Vegetation Map of the People's Republic of China* (1:1 000 000), pp. 10–24, Geological Publishing House, Beijing, China.
- Ellwood, E. R., S. A. Temple, R. B. Primack, N. L. Bradley, and C. C. Davis (2013), Record-breaking early flowering in the eastern United States, *PLoS one*, 8(1), e53788, doi:10.1371/journal.pone.0053788.
- Fang, X., L. Xiao, Q. Ge, and J. Zheng (2005), Changes of plants phenophases and temperature in spring during 1888–1916 around Changsha and Hengyang in Hunan province, *Quat. Sci.*, 25(1), 74–79.

- Ge, Q., J. Zheng, X. Fang, X. Zhang, P. Zhang, Z. Man, and W.-C. Wang (2003), Winter half-year temperature reconstruction for the middle and lower reaches of the Yellow River and Yangtze River, China, during the past 2000 years, *The Holocene*, 13(6), 933–940.
- Gibbins, R. P. (1991), Some effects of precipitation patterns on mesa dropseed phenology, *J Range Manage*, 44(1), 86–90.
- Gong, G., P. Zhang, and J. Zhang (1984), The variation of phenodate in Beijing district, *Chinese Sci Bull*, 29(12), 1650–1652.
- Gonsamo, A., J. M. Chen, and C. Wu (2013), Citizen science: Linking the recent rapid advances of plant flowering in Canada with climate variability, *Sci Rep-UK*, 3(2239), 1–5.
- Häkkinen, R., T. Linkosalo, and P. Hari (1995), Methods for combining phenological time series: Application to bud burst in birch (*Betula pendula*) in Central Finland for the period 1896–1955, *Tree Physiol.*, 15(11), 721–726.
- Hameed, S., and G. Gong (1994), Variation of spring climate in lower-middle Yangtse River Valley and its relation with solar-cycle length, *Geophys. Res. Lett.*, 21(24), 2693–2696.
- Ho, C. H., E.-J. Lee, I. Lee, and S.-J. Jeong (2006), Earlier spring in Seoul, Korea, *Int. J. Climatol.*, 26(14), 2117–2127.
- Holopainen, J., S. Helama, H. Lappalainen, and H. Gregow (2013), Plant phenological records in northern Finland since the 18th century as retrieved from databases, archives and diaries for biometeorological research, *Int. J. Biometeorol.*, 57(3), 423–435.
- IPCC (2007), Summary for policymakers, in *Climate Change 2007: Impacts, Adaptation and Vulnerability. Contribution of Working Group II to the Fourth Assessment Report of the Intergovernmental Panel on Climate Change*, edited by S. Solomon et al., pp. 7–22, Cambridge Univ. Press, Cambridge, U. K.
- Jeong, S. J., C.-H. Ho, H.-J. Gim, and M. E. Brown (2011), Phenology shifts at start vs. end of growing season in temperate vegetation over the Northern Hemisphere for the period 1982–2008, *Global Change Biol*, 17(7), 2385–2399.
- Jolly, W. M., R. Nemani, and S. W. Running (2005), A generalized, bioclimatic index to predict foliar phenology in response to climate, *Global Change Biol*, 11(4), 619–632.
- Jones, P. D., D. H. Lister, T. J. Osborn, C. Harpham, M. Salmon, and C. P. Morice (2012), Hemispheric and large-scale land-surface air temperature variations: An extensive revision and an update to 2010, *J. Geophys. Res.*, 117, D05127, doi:10.1029/2011JD017139.
- Körner, C., and D. Basler (2010), Phenology under global warming, *Science*, 327(5972), 1461–1462.
- Liang, L., M. D. Schwartz, and S. Fei (2011), Validating satellite phenology through intensive ground observation and landscape scaling in a mixed seasonal forest, *Remote Sens. Environ.*, 115(1), 143–157.
- Matsumoto, K., T. Ohta, M. Irasawa, and T. Nakamura (2003), Climate change and extension of the *Ginkgo biloba* L. growing season in Japan, *Global Change Biol*, 9(11), 1634–1642.
- Memmott, J., P. G. Craze, N. M. Waser, and M. V. Price (2007), Global warming and the disruption of plant-pollinator interactions, *Ecol. Lett.*, 10(8), 710–717.
- Menzel, A. (2000), Trends in phenological phases in Europe between 1951 and 1996, *Int. J. Biometeorol.*, 44(2), 76–81.
- Menzel, A. (2003), Plant phenological anomalies in Germany and their relation to air temperature and NAO, *Clim. Change*, 57(3), 243–263.
- Menzel, A., et al. (2006), European phenological response to climate change matches the warming pattern, *Global Change Biol*, 12(10), 1969–1976.
- Michaelsen, J. (1987), Cross-validation in statistical climate forecast models, *J. Climate Appl. Meteorol.*, 26(11), 1589–1600.
- Miller-Rushing, A. J., and R. B. Primack (2008), Global warming and flowering times in Thoreau's Concord: A community perspective, *Ecology*, 89(2), 332–341.
- Morice, C. P., J. J. Kennedy, N. A. Rayner, and P. D. Jones (2012), Quantifying uncertainties in global and regional temperature change using an ensemble of observational estimates: The HadCRUT4 data set, *J. Geophys. Res.*, 117, D08101, doi:10.1029/2011JD017187.
- Peñuelas, J., I. Filella, X. Zhang, L. Llorens, R. Ogaya, F. Lloret, P. Comas, M. Estiarte, and J. Terradas (2004), Complex spatiotemporal phenological shifts as a response to rainfall changes, *New Phytol.*, 161(3), 837–846.
- Peñuelas, J., T. Rutishauser, and I. Filella (2009), Phenology feedbacks on climate change, *Science*, 324(5929), 887–888.
- Reich, P. B. (1995), Phenology of tropical forests: Patterns, causes, and consequences, *Can. J. Bot.*, 73(2), 164–174.
- Rosenzweig, C., et al. (2008), Attributing physical and biological impacts to anthropogenic climate change, *Nature*, 453(7193), 353–357.
- Rutishauser, T. (2009), Historical phenology in central Europe: Seasonality and climate during the past 500 years, *Geogr. Bernensia*, 82, 152.
- Rutishauser, T., J. Luterbacher, F. Jeanneret, C. Pfister, and H. Wanner (2007), A phenology-based reconstruction of interannual changes in past spring seasons, *J. Geophys. Res.*, 112, G04016, doi:10.1029/2006JG000382.
- Schaber, J., and F. W. Badeck (2002), Evaluation of methods for the combination of phenological time series and outlier detection, *Tree Physiol.*, 22(14), 973–982.
- Schaber, J., and F. Badeck (2005), Plant phenology in Germany over the 20th century, *Reg Environ Change*, 5, 37–46.
- Stöckli, R., T. Rutishauser, I. Baker, M. A. Liniger, and A. S. Denning (2011), A global reanalysis of vegetation phenology, *J. Geophys. Res.*, 116, G03020, doi:10.1029/2010JG001545.
- Studer, S., R. Stöckli, C. Appenzeller, and P. L. Vidale (2007), A comparative study of satellite and ground-based phenology, *Int J Biometeorol*, 51(5), 405–414.
- Walther, G. R. (2003), Plants in a warmer world, *Perspect Plant Ecol*, 6(3), 169–185.
- Walther, G., E. Post, P. Convey, A. Menzel, C. Parmesan, J. C. Trevor, J.-M. F. Beebee, O. Hoegh-Guldberg, and F. Bairlein (2002), Ecological responses to recent climate change, *Nature*, 416(6879), 389–395.
- Wang, H., J. H. Dai, and Q. S. Ge (2012), The spatiotemporal characteristics of spring phenophase changes of *Fraxinus chinensis* in China from 1952 to 2007, *Sci. China Earth Sci.*, 55(6), 991–1000.
- Webb, L. B., P. H. Whetton, and E. W. R. Barlow (2011), Observed trends in winegrape maturity in Australia, *Global Change Biol*, 17(8), 2707–2719.
- Wilczek, A. M., L. T. Burghardt, A. R. Cobb, M. D. Cooper, S. M. Welch, and J. Schmitt (2010), Genetic and physiological bases for phenological responses to current and predicted climates, *Philos Trans R. Soc B*, 365(1555), 3129–3147.
- Zhang, X., D. Tarpley, and J. T. Sullivan (2007), Diverse responses of vegetation phenology to a warming climate, *Geophys. Res. Lett.*, 34, L19405, doi:10.1029/2007GL031447.
- Zheng, J., L. Ding, Z. Hao, and Q. Ge (2012), Extreme cold winter events in southern China during AD 1650–2000, *Boreas*, 41(1), 1–12.
- Zheng, J., S. Zhong, Q. Ge, Z. Hao, X. Zhang, and X. Ma (2013), Changes of spring phenodates in Yangtze River Delta Region in the past 150 years, *J Geogr Sci*, 23(1), 31–44.
- Zhu, K. (1973), A preliminary study on the climate fluctuation during the last 5000 years in China, *Sci. Sin.*, 16(2), 226–256.